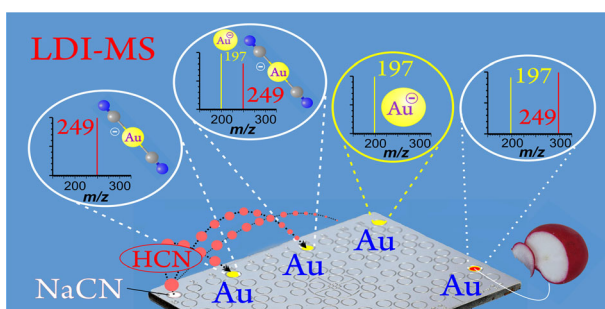


Gold Nanoparticles (AuNPs) as Reactive Matrix for Detection of Trace Levels of HCN in Air by Laser Desorption/Ionization Mass Spectrometry (LDI-MS)

Julius Pavlov, Athula B. Attygalle 

Center for Mass Spectrometry, Department of Chemistry and Chemical Biology, Stevens Institute of Technology, Hoboken, NJ 07030, USA



Abstract. Under direct laser desorption/ionization mass spectrometric conditions, the irradiation of target spots made of gold nanoparticle residues generates a series of peaks at m/z 197, 394, 591... representing Au_n^- ions ($n=1-3$). In contrast, spectra recorded from gold nanoparticles directly mixed with an alkali cyanide exhibited an additional peak at m/z 249, indicating an abundant generation of gaseous $[Au(CN)_2]^-$ ions upon irradiation. The relative intensity of the m/z 249

peak surged when the amount of cyanide in the mixture was increased. Most remarkably, a peak at m/z 249 was observed even from *neat* AuNPs upon irradiation, if a nearby spot, which was not irradiated, happened to bear a cyanide sample. We postulated that traces of HCN emanating from the headspace of aqueous cyanide solution during the sample-plate preparation is sufficient to convert gold to AuCN, which is subsequently detected as $[Au(CN)_2]^-$. Further experiments demonstrated that the relative intensity of the m/z 249 peak diminishes exponentially as the AuNP spot becomes more distant from the putative HCN source. Eventually, the method was developed as an efficient procedure to detect HCN or alkali cyanides. Using KCN, the detection limits were determined to be below 10 pg of CN^- per spot. The method also demonstrated that, upon crushing, the seeds or roots of certain fruits and vegetables such as apple, peach, radish, and cassava, but not carrot, release HCN in amounts detectable by this method.

Keywords: Gold nanoparticles, Laser desorption/ionization mass spectrometry, Reactive matrix, Hydrogen cyanide, AuNPs, Cyano complexes, Cyanogenic compounds, Amygdalin

Received: 26 October 2018/Revised: /Accepted: 28 December 2018/Published Online: 7 March 2019

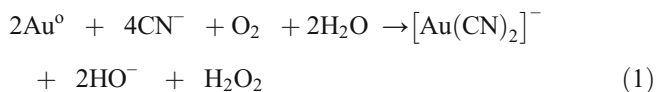
Introduction

Gold is one of the “noble metals,” generally found in nature in its elemental state. In addition to its paramount place in the jewelry industry, gold has many uses in electronics manufacturing and other industrial processes. In 1887, MacArthur and the Forrest Brothers used cyanide to dissolve gold [1]. For the dissolution process to occur,

oxygen and water are also required as reactants. In this redox process, oxygen removes an electron from each gold atom, and the complex $Au(CN)_2^-$ is formed. The cyanide leaching technique can also be used for the detection of elemental gold at very low levels in ores [2]. For quantification, the solutions obtained by leaching are measured by atomic absorption spectrometry [3]. Alternatively, gold can be detected at trace levels by FIA-ICP-MS [4], laser ablation-ICP mass spectrometry [5], or electrospray ionization of complexes made with polydentate nitrogen bases [6]. During the cyanidation process, insoluble AuCN, when in contact with a solution containing excess cyanide ions, tends to accept an extra cyanide group to attain a preferred coordination number, and form the soluble $[Au(CN)_2]^-$.

Electronic supplementary material The online version of this article (<https://doi.org/10.1007/s13361-018-02131-0>) contains supplementary material, which is available to authorized users.

Correspondence to: Athula Attygalle; e-mail: athula.attygalle@stevens.edu



Since colloidal gold, now fashionably called gold nanoparticles (AuNPs), was first made by Faraday in 1857 [7], it has found many applications [8, 9]. More recently, many uses of AuNPs in mass spectrometric analytical procedures have been described [10–19]. One distinct advantage of using of AuNPs for LDI-MS is the inverted NP-to-analyte ratio compared to the excessive amounts of matrix used for traditional MALDI. Uses of AuNPs for LDI-MS include protein quantification [20] and visualization of the spatial distribution of low-molecular-weight compounds in garlic [21].

Hydrogen cyanide is a highly toxic naturally occurring compound present in minute quantities even in common foodstuffs, such as almonds, mangoes, and rapeseed [22]. Certain plants and arthropods release HCN as a defensive chemical against enemy attacks [22–25]. Moreover, cyanides are widely used for chemical synthesis and noble-metal mining [26]. Analytical chemists are interested in detection methods for HCN and other cyanides because of their profound toxicity. Reviews by Linsay et al. [27], Ma and Dasgupta [28], and Randviir and Banks [26] describe the array of methods available for the detection of HCN and cyanides. Moreover, US EPA has several methods recommended for cyanide determination [29–31]. Although these methods achieve detection limits required for regulatory needs, most of them are complex and time-consuming, and require the manipulation of large samples. The application of mass spectrometric methods can alleviate many of the issues related to the selectivity and specificity. Some of the mass spectrometric methods that have been employed for cyanide detection are GC-MS [32–35], LC-MS [36, 37], proton-transfer-reaction mass spectrometry (PTR-MS) [38], and selected-ion flow-tube mass spectrometry (SIFT-MS) [39–41] procedures. A recent innovative approach for trace-level detection of anions is paired-ion electrospray ionization (PIESI) mass spectrometry [42–45]. In this procedure, a dicationic reagent such as 1,1'-(nonane-1,9-diyl)bis(3-methyl-1*H*-imidazol-3-ium) ion is allowed to pair with anions transferred to the gas phase by electrospray ionization. The cationic complexes formed in this way are then determined by mass spectrometry. By this method, cyanide has been detected at picogram levels [43]. In another noteworthy ESI-MS method for cyanide detection, the ion was subjected to react with NaAuCl₄ to form the dicyanogold anion, which was then solvent-extracted and determined as [Au(CN)₂][−] by a selected-reaction monitoring experiment [46, 47]. In an indirect manner, gold nanodots (AuNDs) have been used as a probe for cyanide detection by monitoring the fluorescence signal emitted by AuNDs capped with trithiocyanuric acid (TCA), which can be quenched quantitatively by cyanide ions [48].

Laser desorption/ionization mass spectrometry (LDI-MS) provides a potent way to analyze solid deposits [49]. Many inorganic materials are particularly amenable to analysis by

LDI-MS [50–56]. Previously, laser-induced breakdown spectroscopy (LIBS) coupled with LDI-MS has been used to determine the composition of gold alloys [57]. Previously, AuNP-assisted LDI-MS has been used to determine a variety of analytes [15, 58]. Gold nanoparticle-modified cellulose membranes have been used to selectively determine inorganic ions such as iodide [59], arsenite (AsO₂[−]) [60], and lead [61].

During our mass spectrometric explorations with AuNPs, we serendipitously noticed that elemental gold and alkali-cyanide mixtures generate abundant [Au(CN)₂][−] ions upon laser irradiation. Herein, we describe an adaptation of the procedure for detecting trace amounts of HCN in air and solution by negative-ion LDI-MS.

Experimental

Materials

Sodium cyanide (99.0%), potassium cyanide (99.9%), and sodium citrate (tribasic) dihydrate (ACS reagent) were purchased from Sigma-Aldrich Co. (St. Louis, MO, USA). Tetrachloroauric(III) acid trihydrate (HAuCl₄·3H₂O, ACS reagent) was purchased from Acros Organics (Thermo Fisher Scientific, Waltham, MA, USA). Gold flakes suspended in water were purchased from the National Natural History Museum store at the Smithsonian Institution (Washington, DC). AuNPs were synthesized by the procedure described in Bastús et al. [62]. Briefly, sodium citrate solution (2.2 mM, 15.0 mL) in Millipore water was boiled while stirring, and HAuCl₄ (25 mM, 100 μL) was added (the color of the solution changed from yellow to pink within 10 min, and then to stable purple). The ~10 nm size NPs coated with citrate ions prepared in this way (about 3 × 10¹² particles mL^{−1}, or about 200 μM) were used in all subsequent experiments without further modification [AuNP solution (colloidal gold) prepared in this way was stable for about 9 weeks at room temperature, without the need for any pH adjustments. However, coagulation into visible clumps up to 0.5 cm in diameter was noted after about 10 weeks].

Analysis by Mass Spectrometry

LDI-MS experiments were conducted on a SYNAPT G2 MALDI-ToF mass spectrometer (Waters, Milford, MA, USA) equipped with a solid-state 355-nm Nd:YAG laser (pulse repetition frequency 1000 Hz). Negative-ion LDI-MS and MS/MS data were recorded in the resolution mode (15,000 resolving power at *m/z* 208) over a range of *m/z* 50 to 1000 using the MassLynx 4.1 software (Waters Corp., Milford, MA, USA). Prior to analysis, the mass scale of the instrument was calibrated using ions generated from red phosphorus [63]. The energy of the laser beam was adjusted to obtain optimum ion yield (typical setting 500 arbitrary units). The LDI source was operated with the sample plate at 10 V and extraction voltage at 10 V. For each sample, full-scale MS¹ spectra were acquired by moving the target plate on a pre-programmed spiral scan path

(with a scan duration of 0.5 s, and an overall cycle time of 0.524 s) from one sample location to the next. Data were acquired over a period of 5 min when using a 96-spot plate, or for 2 min when using a 384-spot plate.

For the initial experiments, negative-ion LDI-MS spectra were recorded from deposits made by drying (typically for 20–40 min) of aqueous suspensions of AuNP (2.5 μL) or minuscule gold flakes (2.5 μL) in water, on a stainless-steel MALDI sample plate. Subsequent spectra were recorded from dried residues prepared by evaporating an aqueous NaCN solution (2.5 μL , 10 mM) added to pre-dried Au spots. Analogously, spectra were recorded from neat AuNPs or gold-flake spots that had been inadvertently exposed to HCN vapors because some spots at nearby locations on the same plate contained aliquots of aqueous NaCN solution (2.5 μL , 10 mM) when the plate was dried. Subsequently, a deliberate experiment was conducted to verify the effect of the presence of nearby NaCN spots. Initially, spectra were recorded from a row of dried spots made by evaporating aqueous AuNP suspensions (2.5 μL) inside a vacuum desiccator for 2 h. Afterwards, the plate (plate 1) was removed from the mass spectrometer, and a series of fresh spots of aqueous AuNPs was applied to a new row. Then, a new plate (plate 2) was placed on top of plate 1 (see Supplementary Figures 1 and 2), and aliquots of an aqueous NaCN (5%, 2.5 μL) solution were applied to a row of spots on plate 2. Both plates as an assembly were then placed in a desiccator and vacuum-dried for 2 h. Afterwards, plate 2 was removed, and mass spectra were acquired from both series of dried gold deposits on plate 1.

Analogously, spectra were recorded from a small gold flake deposited dry and allowed to stand dry next to an evaporating drop of NaCN solution on a neighboring sample spot, and from a similar gold-flake sample deposited wet next to a drop of NaCN-solution spot and allowed to dry simultaneously.

To study the distal influence of HCN vapor on gold in more detail, AuNP samples (2.5 μL) were deposited on a series of sample spots separated equidistantly from the top opening of a small (0.5 mm) conical hole that was present on the stainless-steel plate (see Figure 3). The distances from the center of the opening to the center of to each consecutive AuNP sample spot were 3.0, 9.5, 16.0, 22.5, and 29.0 mm. First, AuNP samples were deposited on each spot and allowed to dry in open air at room temperature for 40 min; then, the plate was inverted, and an aliquot of the NaCN solution (10 μL , 10 mM) was placed at the bottom of the conical hole (wide part of the cone). The plate was inverted again and placed face up in a covered plastic storage box; the NaCN solution was allowed to dry overnight. Three series of experimental measurements were conducted on different days. The intensity ratios of the m/z 249 and m/z 197 peaks [for $[\text{Au}(\text{CN})_2]^-$ and Au^- , respectively] were calculated for each spot and the average intensity ratio ($N=3$) was plotted against sample-spot distance from the cyanide deposit. Statistical analysis of the results was performed using SigmaPlot 10.0 (Systat Software, Inc., San Jose, CA USA, www.systatsoftware.com).

Limit of Detection and Quantification

To determine a limit of detection for cyanide using this method, a series of KCN solutions of different concentrations ranging from 1×10^{-7} M to 1×10^{-2} M, in tenfold increments, were made (KCN was selected instead of NaCN for all quantification experiments because of its higher purity). From each KCN solution, 2.5 μL aliquots were mixed with a fixed amount of AuNPs (2.5 μL of 200 μM suspension; equivalent to 5×10^{-12} mol or about 100 ng Au) in triplicate on a stainless-steel MALDI sample plate to deposits of CN^- ranging from 6.5 pg to 650 ng. The plate was allowed to dry for 40 min, and negative-ion spectra were recorded over a narrow mass range (m/z 100 to 300) under the Sensitivity acquisition mode. From the data obtained, a plot of the intensity ratio of m/z 249, $[\text{Au}(\text{CN})_2]^-$, to m/z 197, Au^- , peaks was plotted against the logarithm of the amount of cyanide (in grams) deposited on each spot.

Samples of Plant Origin

Radish juice was freshly squeezed from the root of the vegetable by crushing a piece of it in a mortar. An aliquot of the juice (2.0 μL) was directly transferred to a sample spot pre-coated with dried AuNPs (made from 2.5 μL of the suspension), and allowed to dry. Analogously, small thin slices (about 1.5 mm^2 in area and 200 μm in thickness) were cut with a razor blade from the cores of fresh apple seeds, peach pips, carrot, and a cassava root. The cut tissues were placed directly onto MALDI sample spots pre-coated with dried AuNPs (2.5 μL), kept in contact with the AuNPs for 15 min, removed, and the sample spots were analyzed by LDI-MS immediately.

Results and Discussion

Negative-ion mass spectra recorded from dry deposits made from gold flakes, upon laser irradiation, did not exhibit any significant peaks other than those representing background ions (Figure 1c). However, spectra acquired from spots made from AuNPs showed a series of peaks at m/z 197, 394, and 591, representing Au^- , Au_2^- , and Au_3^- , ions, respectively (Figure 1a). In stark contrast, the spectra recorded from Au and NaCN mixtures showed an approximately 100-fold increase in signal intensity (Figure 1b). More interestingly, a completely new set of peaks were observed at m/z 249, 472, 695, and 918 for a series of $[\text{Au}(\text{CN})_n]^-$ ($n=1-4$) ions (Figure 1b, d). The m/z 249 ion for $[\text{Au}(\text{CN})_2]^-$ has been generated previously under electrospray ionization from reaction mixtures of NaAuCl_4 and cyanide ions [46, 47]. To the best of our knowledge, the generation of $[\text{Au}(\text{CN})_2]^-$ ion under LDI-MS conditions has not been reported previously.

The identification of $[\text{Au}(\text{CN})_n]^-$ ions was confirmed by tandem mass spectrometry. For example, the collision-induced dissociation (CID) performed in the Trap region of a Synapt G2 mass spectrometer revealed that the m/z 249 is a relatively stable ion that fragments only upon quite high ion-activation conditions (30 eV) by a loss of a 223 Da AuCN unit

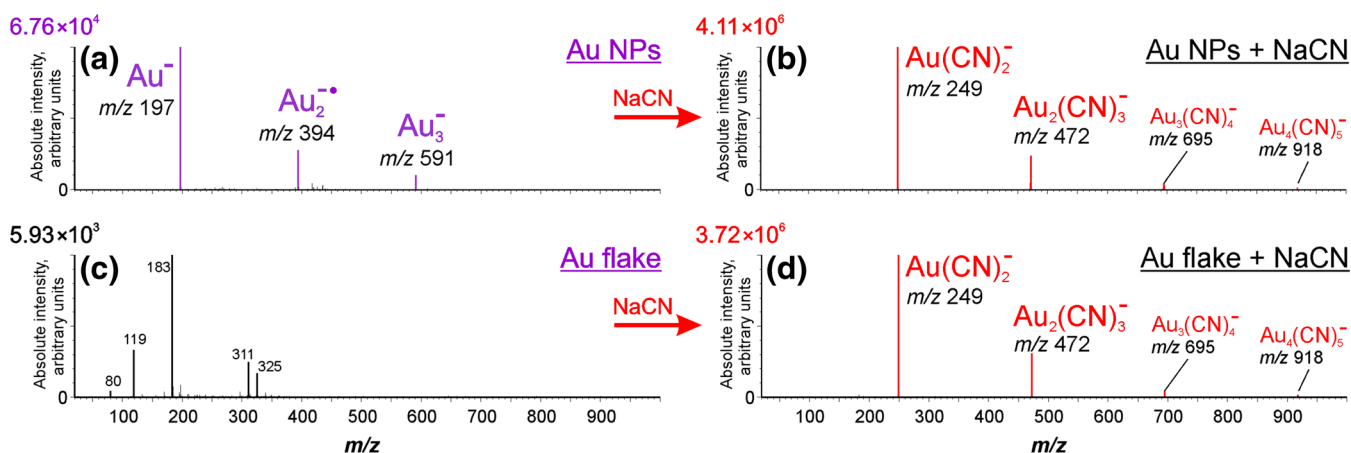


Figure 1. Negative-ion LDI-MS spectra recorded from a dried deposit of AuNPs (a) or a gold-flake suspension (c). The spectra in panels (b) and (d) were recorded from deposits made by drying for 20 min of an aliquot of NaCN solution added to a pre-dried AuNP or a gold-flake spot, respectively

to yield the cyanide anion (m/z 26) (Supplementary Figure 3b) [46]. Thus, the m/z 249 peak was recognized to represent the $[\text{Au}(\text{CN})_2]^-$ ion. The formation of $[\text{Au}(\text{CN})_2]^-$ ion from the interaction of cyanide with TCA-AuNDs has been confirmed previously by ESI-MS by Vasimalai and Fernandez-Arguelles [48]. The dimeric m/z 472 ion, on the other hand, fragmented readily even at 15 eV activation and produced an ion of m/z 249 for $[\text{Au}(\text{CN})_2]^-$ by losing a AuCN unit (223 Da) (Supplementary Figure 3a). In addition, the product-ion spectrum of the m/z 472 ion also showed a low-intensity peak at m/z 275, which represented a minor fragmentation pathway of losing an Au atom to yield the radical-anion $[\text{Au}(\text{CN})_3]^-$. Thus, the m/z 472 ion was recognized as $[\text{Au}_2(\text{CN})_3]^-$. Analogously, the m/z 695 and 918 peaks were recognized to represent $[\text{Au}_3(\text{CN})_4]^-$ and $[\text{Au}_4(\text{CN})_5]^-$, respectively.

While conducting these LDI-MS experiments, we found that under certain conditions, the spectra recorded even from neat AuNPs sometimes showed a peak at m/z 249. Even after taking meticulous care to avoid physical cross-contamination, we continued to see a peak from time to time at m/z 249. We envisaged that this intriguing result might be due to the formation of AuCN that could have occurred during the sample-plate preparation by traces of HCN emanating from adjacent spots where aqueous cyanide solution had been deposited. To test our hypothesis, we recorded LDI-MS spectra from a neat AuNP suspension allowed to evaporate adjacent to a dried NaCN spot. The spectrum showed the base peak at m/z 249 (Figure 2a). Moreover, the intensity of the m/z 249 peak increased 100-fold if the AuNPs had been allowed to dry next to a concomitantly drying NaCN/ H_2O spot (Figure 2b). Furthermore, the intensity of the m/z 249 peak increased even more when the AuNPs deposited next to an aqueous NaCN spot had been allowed to stand for 1 day before the analysis, rather than recording the spectrum immediately after the sample was sufficiently dry. These results supported the proposition that ultra-trace amounts of HCN vapors released from NaCN/ H_2O deposits drying

alongside were sufficient to react with gold nanoparticles and produce a signal at m/z 249, upon laser irradiation.

Apparently, the reaction of Au with cyanide occurs invariably when AuNPs are mixed with NaCN on the same spot on a sample plate, or when aqueous NaCN is present on a

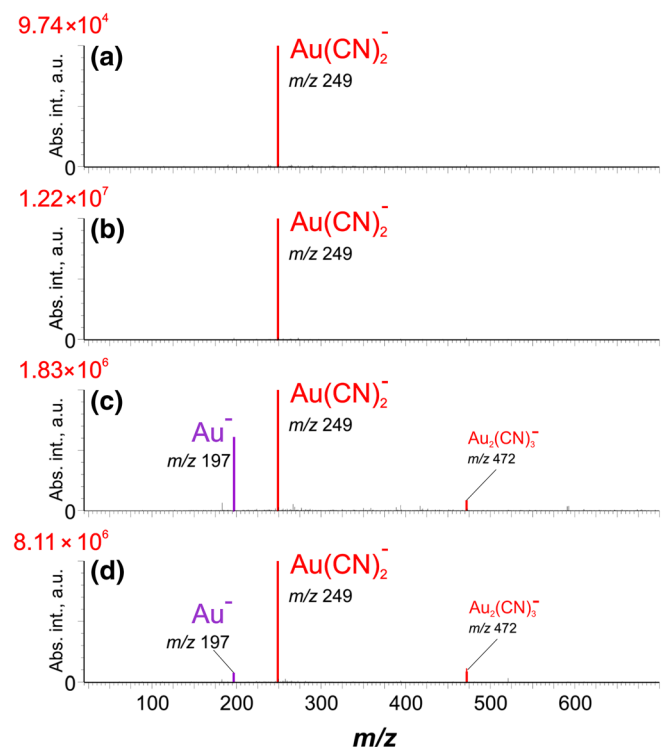


Figure 2. Negative-ion LDI-MS spectra recorded from a drop of aqueous AuNP suspension allowed to evaporate adjacent to a dry NaCN spot (a), from a drop of aqueous AuNPs allowed to dry next to a concomitantly drying aqueous NaCN spot (notice the enhancement of signal intensity) (b), from a dry spot of AuNPs deposited next to an aqueous NaCN spot and allowed to dry, and the sample was analyzed immediately (c), and a dry spot of AuNPs next to a NaCN spot deposited, and analysis performed after 1 day (d)

neighboring or nearby spot. In fact, even gold flakes, which by themselves did not produce significant MS signals, generated intense peaks in spectra recorded after they were placed in water, next to a drop of 5% NaCN solution, and allowed to dry simultaneously (Supplementary Figure 4).

To confirm that the observed contamination takes place via gaseous HCN transfer rather than slow leaching of the solution on the target plate, we applied a NaCN solution to a separate target plate from the one carrying the gold spots (Supplementary Figure 1). Samples on the two plates were allowed to dry in a desiccator simultaneously under vacuum. After separating the plate that carried NaCN, spectra were recorded from the gold deposits. Interestingly, only the spectra from residues from aqueous AuNP deposits that had been allowed to dry simultaneously next to the plate with aqueous NaCN deposits showed a peak at m/z 249 for $[\text{Au}(\text{CN})_2]^-$ (Supplementary Figure 2). The spectra from the gold deposits that had already been dry did not show the m/z 249 peak (Supplementary Figure 2b). This result confirmed that the supply of HCN for the formation of $[\text{Au}(\text{CN})_2]^-$ takes place via an aerial route, even in vacuum.

To study the reaction between AuNPs and HCN in more detail, NP samples were deposited on a series of sample spots arranged consecutively at equal distances away from a small conical hole present on the stainless-steel plate (Figure 3). After AuNPs were dry, the plate was inverted, and a 10 μL aliquot of an aqueous NaCN solution was placed inside the hollow cone.

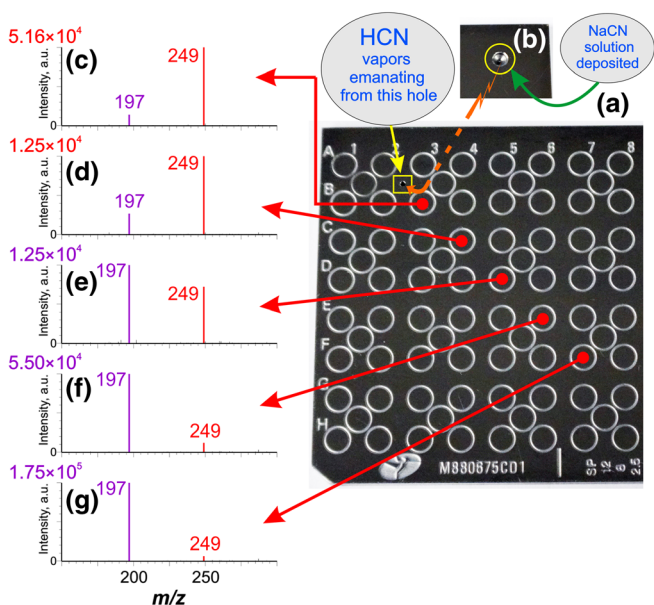


Figure 3. Negative-ion LDI-MS spectra recorded from a drop of aqueous AuNP suspension allowed to evaporate adjacent to a dry NaCN spot (a), from a drop of aqueous AuNPs allowed to dry next to a concomitantly drying aqueous NaCN spot (notice the enhancement of signal intensity) (b), from a dry spot of AuNPs deposited next to an aqueous NaCN spot and allowed to dry, and the sample was analyzed immediately (c), and a dry spot of AuNPs next to a NaCN spot deposited, and analysis was performed after 1 day (d)

After allowing the NaCN drop to dry overnight in an enclosed container, a series of negative-ion LDI-MS measurements were made from each AuNP spot. The spectra recorded from consecutive spots are shown in Figure 3c–g. The intensity ratios of the m/z 249 and m/z 197 peaks, for $[\text{Au}(\text{CN})_2]^-$ and Au^- , respectively, were calculated for each spot, and the averages of the intensity ratios ($N=3$) were plotted against the distance from the hole that acted as the putative HCN-vapor source (Figure 4).

The results showed that the intensity ratio of the m/z 249 and m/z 197 signals for $[\text{Au}(\text{CN})_2]^-$ and Au^- , respectively, diminished exponentially as the distance of the AuNP spot from the hole increased (Figure 4). The result agreed well with that expected from Fick's law of diffusion [64], and thereby supported our hypothesis that the formation of AuCN occurs during sample-plate preparation by gaseous HCN diffusion under ambient conditions. In other words, the amount of cyano-complex formed varies with the distance of the gold to the HCN source in a predictable manner.

Further experiments were conducted to determine the lowest detection limit for cyanide by this procedure. Negative-ion spectra recorded from dried-residue spots made by depositing different amounts of KCN together with a fixed amount of AuNPs, demonstrated that the relative intensity of the m/z 249 peak surges as the amount of KCN is increased (Figure 5). It is well known that MALDI methods are particularly unsuitable for accurate quantitative analyses due to signal variations arising from heterogeneities in the spot composition [65]. Although it may be less acute for the nanoparticle-assisted LDI (NALDI) methods, as the one described here, because of the low NP-to-

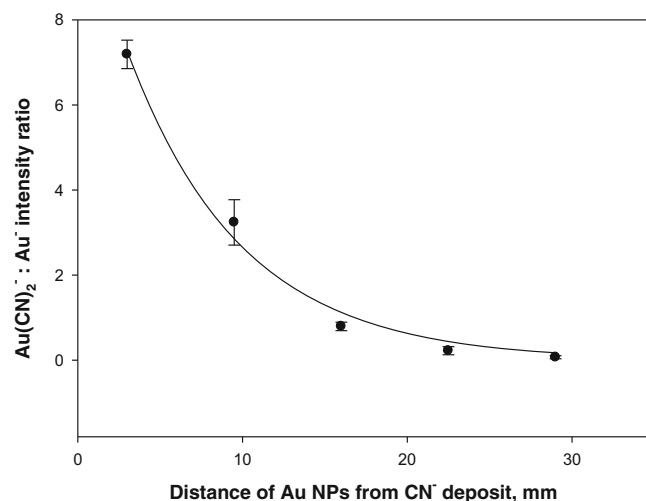


Figure 4. A plot depicting the intensity ratio of the signals m/z 249: m/z 197 for $[\text{Au}(\text{CN})_2]^-$ and Au^- , respectively, acquired from dry deposits of AuNPs (2.5 μL) located at different distances from 10 μL 5% NaCN solution deposited and allowed to evaporate in a pre-drilled hole ($d=0.5$ mm) in the sample plate (shown in Fig. 3). The experiment was conducted in triplicate on different days, using a freshly cleaned sample plate. The intensity ratio displayed a two-parameter exponential-decay relationship with distance ($R^2 = 0.991$)

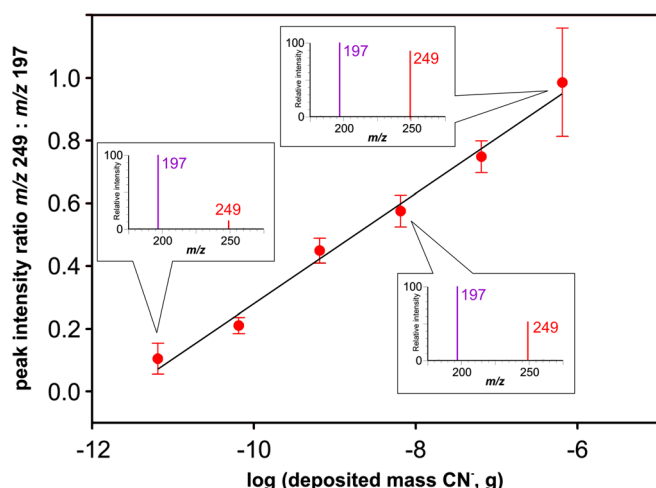


Figure 5. A plot of the intensity ratio of m/z 249 $[\text{Au}(\text{CN})_2]^-$ to m/z 197 $[\text{Au}]^-$ peaks recorded by LDI-MS from residues obtained from different amounts (6.5 pg to 650 ng) of KCN mixed with a fixed amount of AuNPs (2.5 μL of 1.66 μM solution) on a stainless-steel sample plate

analyte ratio and better mixing of the two components, the precision observed is still somewhat low. Even for the mid-value data points with low standard deviations, a relative variance of about 5% was observed (Figure 5). Moreover, we must recognize the fact that gold is not acting as a bona fide internal standard, because it is a reactant participating in the conversion to AuCN. Additionally, the conversion is also not quantitative [Eq. (1)] [66]. Nevertheless, within the range of amounts tested, the intensity ratio of m/z 249 to m/z 197 signals increased exponentially (Figure 5). In this way, the detection limit was determined to be less than 10 pg/spot, which compared well with the values reported from other mass spectrometric methods [43, 46]. Presumably, the extent of the reaction depends on the size of the gold nanoparticles, and on the contact time between gold and cyanide. Moreover, the signal intensities are expected to change with gold nanoparticle size. More importantly, the observed signal intensities can change with instrumental settings and plate-drying conditions. Particularly, the plate voltage was found to exert a pronounced effect. Thus, the curve in Figure 5 is provided only to support the proof of concept that the intensity of the m/z 249 peak depends on the cyanide content. For proper evaluations, a fresh calibration curve must be established under the defined set of conditions used for any particular evaluation.

Finally, spectra were recorded from samples of plant origin: radish, apple seed, peach pip, cassava, and carrot root. Spectra from all samples, except that of carrot, showed a distinct peak at m/z 249 to indicate the presence of cyanide (Figure 6). These results are in excellent agreement with the well-known fact that the seeds of many species of the family *Rosaceae* and parts of the cassava plant contain cyanogenic glycosides (amygdalin in particular). Moreover, monitoring the formation of $[\text{Au}(\text{CN})_2]^-$ by LDI-MS imaging has the potential of becoming a promising method for mapping cyanide-releasing sites in biological tissues.

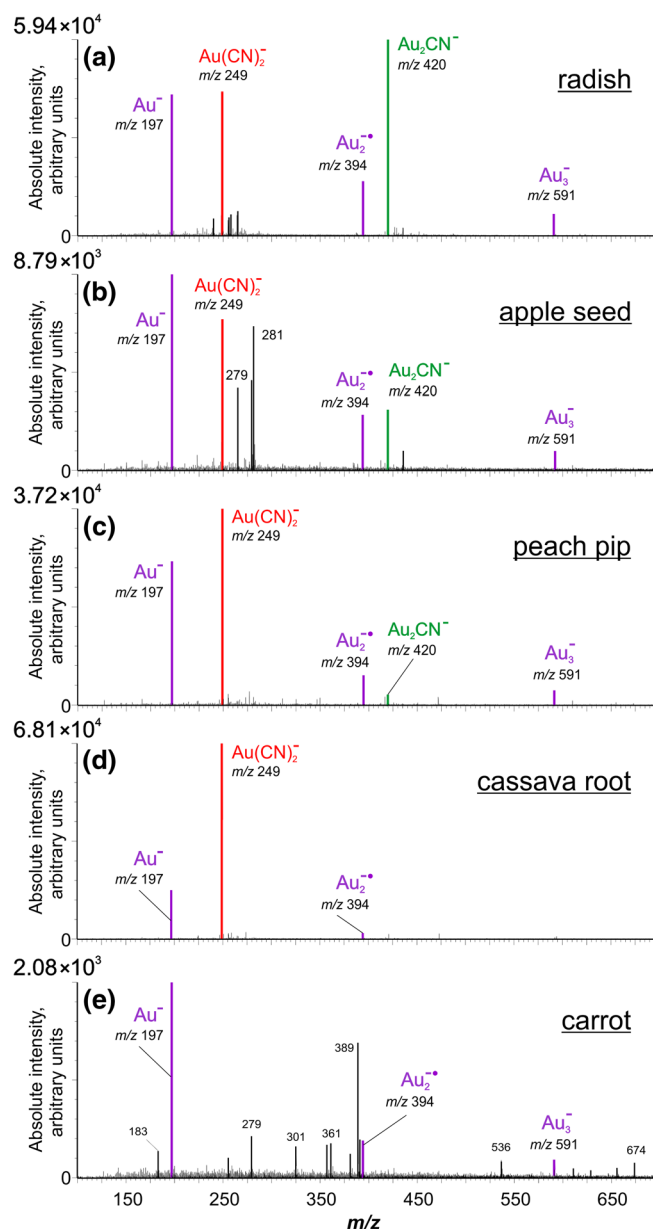


Figure 6. Mass spectrum recorded from a residue of AuNPs (2.5 μL) that had been allowed to dry on a sample spot together with 2.5 μL of freshly squeezed radish juice (a). Analogously, spectra were acquired from AuNPs kept in contact with a sliced apple seed (b), a small piece of sliced peach pip (c), a small piece of sliced cassava root (d), or a small piece of carrot (e). The tissues were kept in contact with dried AuNPs for 15 min, before they were removed and discarded

Conclusions

Many biological samples are known to release trace amounts of HCN [23–26]. Our results show that gold nanoparticles can be used for the rapid, reliable, and sensitive detection of cyanides or cyanogenic compounds in a variety of samples—of chemical or biological origin—in a high-throughput manner using a LDI-MS method. Only a minimum of sample preparation is necessary, and no pre-treatment or derivatization steps are

required. The limits of detection probably depend on a number of factors such as Au particle size and contact time. Although a detailed quantitative study was not conducted, our initial results indicate that a low detection limit of about 10 pg cyanide for solutions is realistic and reproducible. Our results compare favorably, in terms of sensitivity and especially amount of analyte material needed, to other available methods for cyanide detection and quantification such as the ESI-MS-MS method of complexation with NaAuCl₄ to form the dicyanogold anion, which reported a quantification range of 2.6 to 260 µg/L [47]. In contrast, the EPA-recommended method 9014 [29] is effective only above 100-ppb level of free cyanide concentrations. Compared to the EPA method, our procedure or that of Minakata et al. [47] is about 25 times more sensitive. In addition, widely used spectrophotometric methods for cyanide determination [29, 67–74] require milliliter quantities of liquid sample and numerous additional chemicals, and are frequently subject to various chemical interferences. A most valuable feature of our LDI procedure is that it allows for the *direct* analysis of cyanide from complex biological matrices and even when it is not originally present in its free state, with no additional chemicals needed (except for AuNPs).

Finally, an important caveat learned from this study is that, under certain conditions in MALDI work, it is possible that volatiles emanating from samples may not only contaminate neighboring spots, but may in fact *react* with analytes deposited therein. While in our research this has proven to be beneficial, such possible cross-contamination chemistry “through space,” even under vacuum, must be borne in mind in order to avoid misinterpretation of results. Thus, mass spectrometrists should take due precautions during sample preparation. Moreover, it must be borne in mind that gas-phase cross-contaminations in MALDI work could easily occur inside or outside the mass spectrometer when sufficiently volatile and reactive analytes are being used.

Acknowledgements

This work was supported by funds from Stevens Institute of Technology. We thank Dr. Hongjun Wang for the initial gift of gold nanoparticles.

References

- Rubo, A., Kellens, R., Reddy, J., Steier, N., Hasenpusch, W.: “Alkali metal cyanides,” in *Ullmann's Encyclopedia of Industrial Chemistry*. Wiley-VCH, Weinheim (2006)
- Collis, G.D., Moles, C.M.E., Mazaiwana, I.: Exploration for Gold by Use of Cyanide Leach Analytical Techniques on Soil Samples in the Greenstone Belts of Zimbabwe. In: Viewing, K., Dempster, E. (eds.) *African Mining '91*, p. 99. Elsevier, Dordrecht (1991)
- Huffman, Jr. C., Mensik, J.D., Riley, L.B.: Determination of gold in geologic materials by solvent extraction and atomic-absorption spectrometry. Geological Survey Circular 544, U.S. Geological Survey, Washington, D.C., (1968)
- Zhang, Y., Hess, E.V., Pryhuber, K.G., Dorsey, J.G., Tepperman, K., Elder, R.C.: Gold binding sites in red blood cells. *Inorg. Chim. Acta.* **229**, 271–280 (1995)
- Günther, D., Heinrich, C.A.: Enhanced sensitivity in laser ablation-ICP mass spectrometry using helium–argon mixtures as aerosol carrier. *J. Anal. At. Spectrom.* **14**, 1363–1368 (1999)
- Canty, A.J., Colton, R., Thomas, I.M.: Electro spray mass spectrometry of inert and labile metal alkyl compounds: a study of methyl and dimethyl derivatives of gold(III), indium(III) and thallium(III). *J. Organometallic Chem.* **455**, 283–289 (1993)
- Faraday, M.: The Bakerian lecture: experimental relations of gold (and other metals) to light. *Philos. Trans. R. Soc. Lond.* **147**, 145–181 (1857)
- Jellinek, J.: Nanoalloys: tuning properties and characteristics through size and composition. *Faraday Discuss.* **138**, 11–35 (2008)
- Jung, E., Kim, S., Kim, Y., Seo, S.H., Lee, S.S., Han, M.S., Lee, S.: A colorimetric high-throughput screening method for palladium-catalyzed coupling reactions of aryl iodides using a gold nanoparticle-based iodide-selective probe. *Angew. Chem. Int. Ed.* **50**, 4386–4389 (2011)
- Sacks, C.D., Stumpo, K.A.: Gold nanoparticles for enhanced ionization and fragmentation of biomolecules using LDI-MS. *J. Mass Spectrom.* **53**, 1070–1077 (2018)
- McLean, J.A., Stumpo, K.A., Russell, D.H.: Size-selected (2–10 nm) gold nanoparticles for matrix assisted laser desorption ionization of peptides. *J. Am. Chem. Soc.* **127**, 5304–5305 (2005)
- Stumpo, K.A., Russell, D.H.: Anion effects on ionization efficiency using gold nanoparticles as matrices for LDI-MS. *J. Phys. Chem. C.* **113**, 1641–1647 (2009)
- Chau, S.-L., Tang, H.-W., Ng, K.-M.: Gold nanoparticles bridging infrared spectroscopy and laser desorption/ionization mass spectrometry for direct analysis of over-the-counter drug and botanical medicines. *Anal. Chim. Acta.* **919**, 62–69 (2016)
- Castellana, E.T., Russell, D.H.: Tailoring nanoparticle surface chemistry to enhance laser desorption ionization of peptides and proteins. *Nano Lett.* **7**, 3023–3025 (2007)
- Abdelhamid, H.N., Wu, H.-F.: Gold nanoparticles assisted laser desorption/ionization mass spectrometry and applications: from simple molecules to intact cells. *Anal. Bioanal. Chem.* **408**, 4485–4502 (2016)
- Schaaff, T.G.: Metastable ions produced in laser desorption of gold : thiolate cluster compounds. *Rapid Commun. Mass Spectrom.* **17**, 2567–2570 (2003)
- Schaaff, T.G.: Laser desorption and matrix-assisted laser desorption/ionization mass spectrometry of 29-kDa Au : SR cluster compounds. *Anal. Chem.* **76**, 6187–6196 (2004)
- Marsico, A.: Analysis of gold nanoparticles and their use with laser desorption/ionization mass spectrometry, PhD thesis, University of Massachusetts Amherst. (2017) https://scholarworks.umass.edu/dissertations_2/893
- Harkness, K.M., Balinski, A., McLean, J.A., Cliffel, D.E.: Nanoscale phase segregation of mixed thiolates on gold nanoparticles. *Angew. Chem.* **123**, 10742–10747 (2011)
- Ju, S., Yeo, W.-S.: Quantification of proteins on gold nanoparticles by combining MALDI-TOF MS and proteolysis. *Nanotechnology.* **23**, 135701–135707 (2012)
- Misiorek, M., Sekuła, J., Ruman, T.: Mass spectrometry imaging of low molecular weight compounds in garlic (*Allium sativum* L.) with gold nanoparticle enhanced target. *Phytochem. Anal.* **28**, 479–486 (2017)
- Jones, D.A.: Why are so many food plants cyanogenic. *Phytochemistry.* **47**, 155–162 (1998)
- Blum, M.S., Woodring, J.P.: Secretion of benzaldehyde and hydrogen cyanide by the millipede *Pachydesmus crassicutis*. *Science.* **138**, 512–513 (1962)
- Eisner, H.E., Wood, W.F., Eisner, T.: Hydrogen cyanide production in North American and African polydesmoid millipedes. *Psyche A J. of Entom.* **82**, 20–23 (1975)
- Schildknecht, H., Maschwitz, U., Krauss, D.: Blausäure im Wehrsekret des Erdläufers *Pachymerium ferrugineum* XXXV. Mitteilung über Arthropoden-Abwehrstoffe. *Naturwissenschaften.* **55**, 230 (1968)
- Randviir, E.P., Banks, C.E.: The latest developments in quantifying cyanide and hydrogen cyanide. *Trends in Anal. Chem.* **64**, 75–85 (2015)
- Lindsay, A.E., Greenbaum, A.R., O'Hare, D.: Analytical techniques for cyanide in blood and published blood cyanide concentrations from healthy subjects and fire victims. *Anal. Chim. Acta.* **511**, 185–195 (2004)
- Ma, J., Dasgupta, P.K.: Recent developments in cyanide detection: a review. *Anal. Chim. Acta.* **673**, 117–125 (2010)
- United States Environmental Protection Agency (EPA). Cyanide in waters and extracts using titrimetric and manual spectrophotometric procedures. Method 9014 (1996)

30. United States Environmental Protection Agency (EPA). Potentiometric determination of cyanide in aqueous samples and distillates with ion selective electrode. Method 9213, 1996
31. United States Environmental Protection Agency (EPA). Available cyanide by flow injection, ligand exchange and amperometry. Method OIA-1677, 2004
32. Zain, S.M.S.M, Shaharudin, R., Kamaluddin, M.A., Daud, S.F.: Determination of hydrogen cyanide in residential ambient air using SPME coupled with GC-MS. *Atmos. Pollut. Res.* **8**, 678–685 (2017)
33. Murphy, K.E., Schantz, M.M., Butler, T.A., Benner, B.A., Wood, L.J., Turk, G.C.: Determination of cyanide in blood by isotope dilution gas chromatography–mass spectrometry. *Clin. Chem.* **52**, 458–467 (2006)
34. Lobger, L.-L., Petersen, H.W., Andersen, J.E.T.: Analysis of cyanide in blood by headspace-isotope-dilution-GC-MS. *Anal. Lett.* **41**, 2564–2586 (2008)
35. Campanella, B., Biancalana, L., D'Ulivo, L., Onor, M., Bramanti, E., Mester, Z., Pagliano, E.: Determination of total cyanide in soil by isotope dilution GC/MS following pentafluorobenzyl derivatization. *Anal. Chim. Acta.* **961**, 74–81 (2017)
36. Lacroix, C., Saussereau, E., Boulanger, F., Goullé, J.P.: Online liquid chromatography-tandem mass spectrometry cyanide determination in blood. *J. Anal. Toxicol.* **35**, 143–147 (2011)
37. Kang, H.-I., Shin, H.-S.: Derivatization method of free cyanide including cyanogen chloride for the sensitive analysis of cyanide in chlorinated drinking water by liquid chromatography-tandem mass spectrometry. *Anal. Chem.* **87**, 975–981 (2015)
38. Knighton, W.B., Fortner, E.C., Midey, A.J., Viggiano, A.A., Herndon, S.C., Wood, E.C., Kolb, C.E.: HCN detection with a proton transfer mass spectrometer. *Int. J. Mass Spectrom.* **283**, 112–121 (2009)
39. Enderby, B., Smith, D., Carroll, W., Lenney, W.: Hydrogen cyanide as a biomarker for *Pseudomonas Aeruginosa* in the breath of children with cystic fibrosis. *Pediatr. Pulm.* **44**, 142–147 (2009)
40. Gilchrist, F.J., Bright-Thomas, R.J., Jones, A.M., Smith, D., Španěl, P., Webb, A.K., Lenney, W.: Hydrogen cyanide concentrations in the breath of adult cystic fibrosis patients with and without *Pseudomonas aeruginosa* infection. *J. Breath Res.* **7**, 026010–026016 (2013)
41. Španěl, P., Smith, D.D.: Account: on the features, successes and challenges of selected ion flow tube mass spectrometry. *Eur. J. Mass Spectrom.* **19**, 225–246 (2013)
42. Kirk, A.B., Martinelango, P.K., Tian, K., Dutta, A., Smith, E.E., Dasgupta, P.K.: Perchlorate and iodide in dairy and breast milk. *Environ. Sci. Technol.* **39**, 2011–2017 (2005)
43. Soukup-Hein, R.J., Rensburg, J.W., Dasgupta, P.K., Armstrong, D.W.: A general, positive ion mode ESI-MS approach for the analysis of singly charged anions using dicationic reagent. *Anal. Chem.* **79**, 7346–7352 (2007)
44. Xu, C., Guo, H., Breitbart, Z.S., Armstrong, D.W.: Mechanism and sensitivity of anion detection using rationally designed unsymmetrical dications in paired ion electrospray ionization (PIESI) mass spectrometry. *Anal. Chem.* **86**, 2665–2672 (2014)
45. Breitbart, Z.S., Berthod, A., Huang, K., Armstrong, D.W.: Mass spectrometric detection of trace anions: the evolution of paired ion electrospray ionization (PIESI). *Mass Spec. Rev.* **35**, 201–218 (2016)
46. Minakata, K., Nozawa, H., Gonmori, K., Suzuki, M., Suzuki, O.: Determination of cyanide, in urine and gastric content, by electrospray ionization tandem mass spectrometry after direct flow injection of dicyanogold. *Anal. Chim. Acta.* **651**, 81–84 (2009)
47. Minakata, K., Nozawa, H., Gonmori, K., Yamagishi, I., Suzuki, M., Hasegawa, K., Watanabe, K., Suzuki, O.: Determination of cyanide in blood by electrospray ionization tandem mass spectrometry after direct injection of dicyanogold. *Anal. Bioanal. Chem.* **400**, 1945–1951 (2011)
48. Vasimalai, N., Fernandez-Arguelles, M.T.: Novel one-pot and facile room temperature synthesis of gold nanodots and application as highly sensitive and selective probes for cyanide detection. *Nanotechnology.* **27**, 475505 (2016)
49. Muthu, M., Chun, S., Wu, H.-F., Duncan, M.W., Gopal, J.: The ongoing evolution of laser desorption/ionization mass spectrometry: some observations on current trends and future directions. *J. Mass Spectrom.* **53**, 525–540 (2018)
50. Pavlov, J., Attygalle, A.B.: Laser ionization mass spectrometry of inorganic ions, in *Mass Spectrometry Handbook*, ed. M. S. Lee, Wiley, Hoboken, pp. 1207–1227 (2012)
51. Ogundipe, A., Pavlov, J., Braidia, W., Koutsospyros, A., Sen, G., Christodoulatos, C., O'Connor, G.: Evolution of analytical methods to address tungsten speciation. *Global NEST J.* **11**, 308–317 (2009)
52. Pavlov, J., Braidia, W., Ogundipe, A., O'Connor, G., Attygalle, A.B.: Generation and detection of gaseous $W_{12}O_{41}$ and other tungstate anions by laser desorption ionization mass spectrometry. *J. Am. Soc. Mass Spectrom.* **20**, 1782–1789 (2009)
53. Kruegel, A., Attygalle, A.B.: Elemental sulfur as a versatile low-mass-range calibration standard for laser desorption ionization mass spectrometry. *J. Am. Soc. Mass Spectrom.* **21**, 112–116 (2010)
54. Kruegel, A., Pavlov, J., Attygalle, A.B.: Enhancement of laser desorption ionization mass spectrometric signals of CsI by elemental sulfur. *Rapid Commun. Mass Spectrom.* **27**, 763–766 (2013)
55. Zheng, Z., Pavlov, J., Attygalle, A.B.: Detection and imaging of chrome yellow (lead chromate) in latent prints, solid residues, and minerals by laser-desorption-ionization mass spectrometry (LDI-MS). *J. Mass Spectrom.* **52**, 347–352 (2017)
56. Lal, S., Zheng, Z., Pavlov, J., Attygalle, A.B.: Brimstone chemistry under laser light assists mass spectrometric detection and imaging the distribution of arsenic in minerals. *Dalton Trans.* **47**, 8221–8228 (2018)
57. Ahmed, N., Ahmed, R., Baig, M.A.: Analytical analysis of different karats of gold using laser induced breakdown spectroscopy (LIBS) and laser ablation time of flight mass spectrometer (LA-TOF-MS). *Plasma Chem. Plasma Process.* **38**, 207–222 (2018)
58. Alyssa, M.: Analysis of gold nanoparticles and their use with laser desorption/ionization mass spectrometry. *Doctoral Dissertations.* 893 (2017). https://scholarworks.umass.edu/dissertations_2/893
59. Li, Y.-J., Tseng, Y.-T., Unnikrishnan, B., Huang, C.-C.: Gold-nanoparticles-modified cellulose membrane coupled with laser desorption/ionization mass spectrometry for detection of iodide in urine. *ACS Appl. Mater. Interfaces.* **5**, 9161–9166 (2013)
60. Weng, C.-I., Cang, J.-S., Chang, J.-Y., Hsiung, T.-M., Unnikrishnan, B., Hung, Y.-L., Tseng, Y.-T., Li, Y.-J., Shen, Y.-W., Huang, C.-C.: Detection of arsenic(III) through pulsed laser-induced desorption/ionization of gold nanoparticles on cellulose membranes. *Anal. Chem.* **86**, 3167–3173 (2014)
61. Liu, Y.C., Chiang, C.K., Chang, H.T., Lee, Y.F., Huang, C.-C.: Using a functional nanogold membrane coupled with laser desorption/ionization mass spectrometry to detect lead ions in biofluids. *Adv. Funct. Mater.* **21**, 4448–4455 (2011)
62. Bastús, N.G., Comenge, J., Puentes, V.: Kinetically controlled seeded growth synthesis of citrate-stabilized gold nanoparticles of up to 200 nm: size focusing versus Ostwald ripening. *Langmuir.* **27**, 11098–11105 (2011)
63. Sládková, K., Houška, J., Havel, J.: Laser desorption ionization of red phosphorus clusters and their use for mass calibration in time-of-flight mass spectrometry. *Rapid Commun. Mass Spectrom.* **23**, 3114–3118 (2009)
64. Philibert, J.: One and a half century of diffusion: Fick, Einstein, before and beyond. *Diffusion Fundam.* **2**, 1–10 (2005)
65. Wang, P., Giese, R.W.: Recommendations for quantitative analysis of small molecules by matrix-assisted laser desorption ionization mass spectrometry. *J. Chromatogr. A.* **1486**, 35–41 (2017)
66. Habashi, F.: Kinetics and mechanism of gold and silver dissolution in cyanide solution. *Bulletin 59*, State of Montana bureau of mines and geology, Butte, (1967)
67. Validated Test Method 9016: Free cyanide in water, soils and solid wastes by microdiffusion. US EPA Method 9016 (2010)
68. Scoggins, M.W.: Ultraviolet spectrophotometric determination of cyanide ion. *Anal. Chem.* **44**, 1294–1296 (1972)
69. Clyde, D.D., Warner, M.A.: Spectrophotometric determination of cyanide by use of aqueous potassium iodide and mercury(II) iodide. *Analyst.* **103**, 648–651 (1978)
70. Nagashima, S.: Spectrophotometric determination of cyanide with γ -picoline and barbituric acid. *Anal. Chim. Acta.* **91**, 303–306 (1977)
71. Nagashima, S.: Spectrophotometric determination of cyanide with sodium isonicotinate and sodium barbiturate. *Anal. Chim. Acta.* **99**, 197–201 (1978)
72. Nagashima, S., Ozawa, T.: Spectrophotometric determination of cyanide with isonicotinic acid and barbituric acid. *Intern. J. Environ. Anal. Chem.* **10**, 99–106 (1981)
73. Cacace, D., Ashbaugh, H., Kouri, N., Bledsoe, S., Lancaster, S., Chalk, S.: Spectrophotometric determination of aqueous cyanide using a revised phenolphthalein method. *Anal. Chim. Acta.* **589**, 137–141 (2007)
74. Epstein, J.: Estimation of microquantities of cyanide. *Anal. Chem.* **19**, 272–274 (1947)